Pergamon

Progress in Oceanography 55 (2002) 45–64

Progress in Oceanography

www.elsevier.com/locate/pocean

Interannual to interdecadal changes in the Bering Sea and concurrent 1998/99 changes over the North Pacific

S. Minobe [ab,*]

[a] *Division of Earth and Planetary Sciences, Graduate School of Sciences, Hokkaido University, Sapporo 060-0810, Japan*
[b] *Frontier Research System for Global Change, Yokohama, Japan*

Abstract

Sea-Surface Temperatures (SSTs), upper water Heat Storage (HS), Sea-Level Displacements (SLDs), Sea-Ice Concentration (SICs) in the Bering Seas and associated atmospheric circulations are analyzed to identify dominant interannual to interdecadal variations. As a representative time series of the SST variations, Principal Component (PC) of the first mode of a seasonally combined Empirical Orthogonal Function (EOF) is employed. The corresponding EOF (spatial pattern) exhibits the smallest amplitudes in winter and largest in summer. PC1 is characterized by a warming trend throughout the record (1921–2001) with the warmest year in 1997, which is followed by rapid cooling until 1999. The warming from 1995–1997 and cooling from 1997–1999 are commonly found in HS along the southern rim of the Bering Sea, and also accompanied by SLD rise and fall, respectively. The SIC variability corresponding to SST PC1 is prominent in the eastern Bering Sea in spring with correlations as high as 0.7, but good correlations were mainly observed prior to 1990. The correlations between the SST PC1 and sea-level pressures (SLPs) also suggest that the spring atmospheric circulation anomalies play an important role in the variations of the SST and sea-ice in the Bering Sea.

The cooling and SLD fall in the late 1990s in the Bering Sea might be related with a possible major regime shift in 1998/1999, which was discussed by Minobe (2000), Hare and Mantua (2000), and Schwing and Moore (2000). In the 1998/99 change over the North Pacific, SSTs and HS increased abruptly both in the Kuroshio/Oyashio Extension region and the central North Pacific, accompanied by cooling in the eastern North Pacific. At the same time, SLDs rose from Japan to 160°W roughly along Kuroshio Extension path with a tongue-like structure. The tongue-like SLD rise is likely forced by wintertime atmospheric anomalies associated with SLP increase in the eastern North Pacific.

Contents

* Corresponding author. Tel.: +81 11 706 2644; fax: +81 11 746 2715.
E-mail address: minobe@ep.sci.hokudai.ac.jp (S. Minobe).

0079-6611/02/$ - see front matter © 2002 Elsevier Science Ltd. All rights reserved.
PII: S0079-6611(02)00069-1

1. Introduction

Interannual to interdecadal variations in physical environments in the ocean are important scientific topics. Previous studies have shown that Sea–Surface Temperatures (SSTs) and sea-ice distributions in the Bering Sea are influenced by large-scale climate phenomena. Global-scale correlation or regression maps of SSTs with respect to the El Niño/Southern Oscillation (ENSO) indices are to be found in a number of papers (e.g. Zhang, Wallace, & Battisti, 1997; Trenberth & Caron, 2000), regression coefficients with respect to the Pacific Decadal Oscillation Index (PDOI) are also shown in Mantua, Hare, Zhang, Wallace and Francis (1997). The influence of ENSOs on Bering Sea SSTs and sea-ice distributions was studied by Niebauer, 1988, 1998), and Niebauer reported that there had been an abrupt reduction of the sea-ice cover associated with the 1970s climatic regime shift, which was one of the three major climatic regime shifts in the 20th century (Minobe, 1997; Mantua et al., 1997). Although these studies are useful for understanding the regional changes in a context of global climate changes, such approaches may miss substantial regional changes that are not correlated to the variability of the large-scale climate indices. Thus, unless variance explained by such a relation is very high (say $R^2 > 50\%$ or correlation coefficients higher than 0.7), regional changes themselves are worth close examination. The correlation coefficients between SSTs and Sea-Ice Concentrations (SICs) with respect to large-scale climate indices, such as the Southern Oscillation Index (SOI), PDOI, North Pacific Index (NPI), and Arctic Oscillation Index (AOI) are summarized in the Appendix. Although the correlations between the PDOI and SSTs are higher than between the other relations, the variance of the SSTs explained by the PDOI is 10–20% of the total interannual variance. Thus, 80–90% of the total variance remains unexplained by this single climate index.

In the present paper, therefore, we aim to clarify the structure of the major SST changes in the Bering Sea and to identify associated variability in the ocean, ice, and atmosphere, using a wide-range of available datasets with an emphasis on the recent decade. In addition to SSTs and SICs, which were often studied for the Bering Sea, we also analyzed Heat Storages (HSs) (White, 1995) and Sea-Level Displacements (SLDs) observed by Topex/Poseidon (Cheney, Miller, Agreen, Doyle, & Lillibridge, 1994), both of which became available in the 1990s. These new parameters may provide some indications of the oceanic changes at depth.

As will be shown below, the 1990s change in the Bering Sea was characterized by warming and SLD rise from 1995–1997 followed by cooling and SLD fall from 1997–1999. The latter change (referred to as the 1998/99 changes) occurred concurrently with the Pacific-scale atmospheric and oceanic changes, which can be a manifestation of a possible major climatic regime shift with opposing sign to the 1976/77 shift (Minobe, 2000; Hare & Mantua, 2000; Schwing & Moore, 2000; Schwing, Murphree, de Witt & Green, 2002). Because of the importance of the 1998/99 changes as shown by their dramatic occurrences, we also document their structures over the North Pacific.

The present paper is organized as follows. In section 2, data and methodology are explained. The Bering

Sea changes are described in section 3, with subsections of oceanic changes including SST, HS and SLD changes, sea-ice changes, and atmospheric changes represented by SLP changes. The 1998/99 changes over the North Pacific are documented in section 4. The summary and discussion are presented in section 5.

2. Data and method

We analyze the following monthly gridded datasets of SST, SIC, HS, SLD, and SLP. The SST and SIC are provided from the UK Meteorological Office as Global Sea Ice coverage and Sea Surface Temperature data (GISST) version 2.3b, and are produced on a monthly $1° \times 1°$ grid from 1871 to February 2002. The SSTs incorporate ship and satellite observations, estimations from SICs, and interpolations based on Empirical Orthogonal Function (EOF). The SICs are derived from Walsh's (1995) data and GISST 1.1 produced by Parker and Jackson (1995). Detailed methodologies for GISST 2.3β are described by Rayner, Horton, Parker, Folland and Hackett (1996). The HS dataset presented for the upper 400 m from January 1955 to December 2001 is an updated version of White's (1995) dataset, and was estimated by using an optimal interpolation onto a $2° \times 5°$ latitude/longitude grid. The available grids of the HS cover only the southern rim of the Bering Sea, with most of available grids being at 54°N with exception of two 56°N grids in the middle of the basin. Regardless of this limitation, this dataset still provides some insights for Bering Sea changes as we shall see later. The SLD is determined by Topex/Poseidon satellite altimetry and gridded monthly on a $1° \times 4°$ grid (Cheney, Miller, Agreen, Doyle & Lillibridge, 1994). The tidal component was removed using version 3.0 of the Center for Space Research of University of Texas tidal model (Eanes & Bettadpur, 1996). This and other tidal models are expected to have problems in shallow water areas, where the tides become large and spatially complicated (Shum et al., 1997). Thus, the quality of the SLD data over shallow shelf and strait regions can be questionable. The monthly $5° \times 5°$ SLP data from January 1899 to January 2002 was provided from NCAR, and this dataset is an updated version of the SLP data of Trenberth and Paolino (1980).

For the present analysis on interannual variability, it is important to take account of the seasonality of the Bering Sea. Most of the Bering Sea is covered by sea-ice in the winter and spring seasons with its largest extent in March, but in September it is free from sea-ice. This seasonal advance and retreat of sea-ice is the largest for any of the Arctic or subarctic regions (Walsh & Johnson, 1979). These seasonal changes in sea-ice cover may cause seasonal dependencies in other parameters. The Bering Sea SSTs have quite small interannual variance in winter but large variance in summer; the summertime variance being 2.5 times higher than the wintertime variance (interannual variance averaged over 53°–65°N, 160°E–160°W is $0.17°C^2$ in winter and $0.42°C^2$ in summer). In general, SST variances in mid-latitudes also tend to be larger in summer than in winter, since the summertime stratification limits the temperature variations associated with the SST changes within a shallow mixed layer. However, the disparity between the SST variances in the winter and summer is not as large as observed in the Bering Sea; for example the summertime variance at the mid-latitudes in the North Pacific (25°–45°N, 140°E–120°W) is only 1.3 times higher the wintertime variance. This indicates that the summertime variability has relatively larger importance in the Bering Sea than in other North Pacific areas.

The major SST variability in the Bering Sea is examined by a seasonally combined EOF analysis for seasonal mean SST data in the Bering Sea (53°–65°N, 160°E–160°W). For this analysis, we compute EOFs based on a covariance matrix constructed from the yearly time series for each of four seasons at each grid point, with weights proportional to the roots of cosine of latitudes. In other words, different seasons are used as if they are different spatial grids in a conventional EOF. Thus, resultant yearly sampled Principal Components (PCs) or time coefficients are common for four seasons, and seasonal dependencies are expressed in EOFs or spatial pattern, which are given by correlations or regressions of seasonally sampled data at each grid onto the PCs. The seasonally combined EOF was also used by Minobe and Mantua

(1999), and is sometimes called cycle-stationary EOF (Kim & Wu, 2000). The seasonally combined EOF is a useful tool to understand the seasonal dependency of climate variability, especially for cases in which we do not know which season is the most important. Most of Pacific-scale climate analyses have been concentrated on the winter season (Trenberth & Hurrel, 1994), but some papers have studied summertime Bering Sea variability (Overland, Bond, & Adams, 2001). In this paper, winter has been defined as December, January, and February and is labeled by the year for the appropriate January. Likewise, a year is defined as the twelve-month period from December to November and is labeled as the year in which January occurred.

The seasonally combined EOF analysis is also able to identify regions of energetic variability as can conventional EOFs. Consequently, herein we do not a priori limit our attention to a specific season or region in the Bering Sea, but allow the SST data to determine these by themselves. It is noteworthy, however, that in the Bering Sea there is a distinct interregional contrast between the deep basin and shallow shelf areas. Most of previous studies of the Bering Sea have examined the shelf areas, especially southeastern shelf (Stabeno, Schumacher, Davis, & Napp, 1998; Stabeno, Bond, Kachel, Salo, & Schumacher, 2001), since shelf regions are important for marine ecosystem.

The quality of some data, including SST, SIC and SLP may present some problems in the early years when the numbers of observations were small. We check the reliability of the SST data by examining available data distributions (Fig. 1) in UK Metrological Office Historical SST (MOHSST) version 6, which was produced from the same collection of SST ship observations on a monthly $5° \times 5°$ grid without the heavy interpolation employed for the GISST. The MOHSST has missing grids in which observations are lacking, but such grids are estimated from SICs or interpolated using EOFs in the GISST (Rayner, Horton, Parker, Folland & Hackett, 1996). The availability of grids in MOHSST, as expected, continuously increased over the Bering Sea (Fig. 1). There are some available grids through the 20th century centered at 52.5°N, which straddle the southern rim of the Bering Sea and the northern rim of the Pacific Ocean, with more than half of the grids being available after 1921. The observations for these grids, however, may be obtained from the North Pacific rather than the Bering Sea in the first half of the 20th century, only since 1957 (1966) do more than half of grids become available at 57.5°N (62.5°N). The seasonally-combined EOFs are calculated using GISST for three periods, i.e., 1921–2001, 1957–2001, and 1966–2001, during which more than half of grids are available in MOHSST at 52.5°N, 57.5°N, and 62.5°N, respectively. The resultant three PCs are almost identical for overlapping periods as well as the corresponding EOFs, as correlation coefficients between PCs are higher than 0.99. Thus, we use the EOF for the data from 1921 to 2001 in the present paper; the PC in the early period may be regarded an estimate based on SICs or SST observations outside of the Bering Sea, but may still provide some hints for the Bering Sea changes through the 20th century.

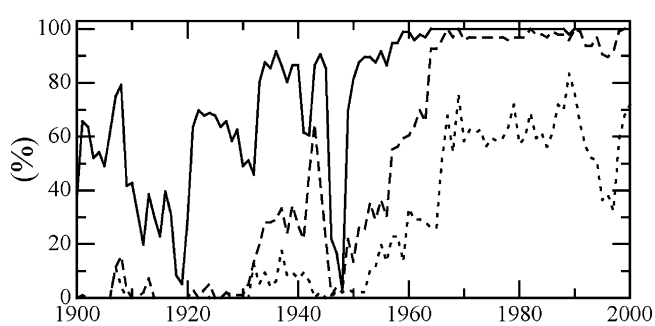

Fig. 1. Percentage of available grid between 160°E–160°W in MOHSST6 with central latitudes at 52.5°N (solid line), 57.5°N (dashed line), and 62.5°N (dotted line).

A visual inspection of the SIC data indicates that the early part of the SIC data is not reliable, because interannual variability before 1954 is quite small. Thus, we use the SIC data after 1955. By taking account of potential problems in SLP data in early periods in high-latitudes noted by Trenberth and Paolino (1980) and consistency with the SIC analysis, we also use the SLP data only after 1955 unless otherwise stated.

3. Changes over the Bering Sea

3.1. Oceanographic changes

Fig. 2 shows the regression coefficients of SSTs over the North Pacific onto the PC1 of the seasonally combined EOF for the Bering Sea (53°–65°N, 160°E–160°W). The first EOF mode explains 43% of the

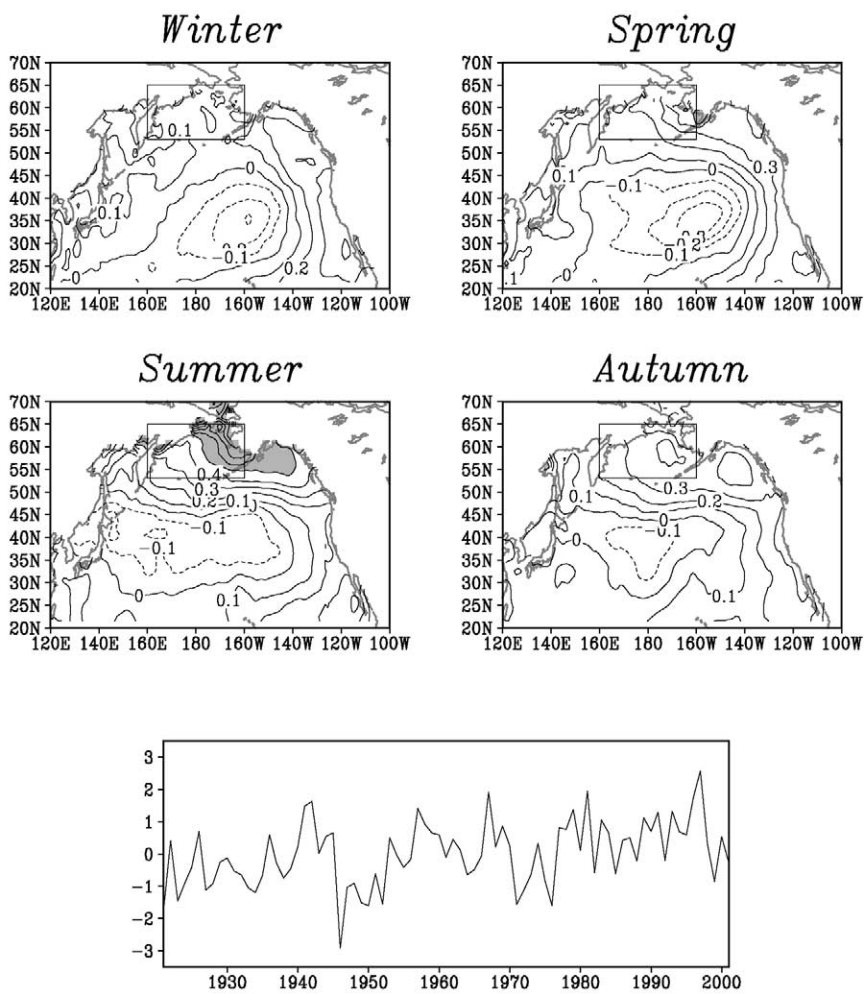

Fig. 2. Regression coefficients of seasonal SSTs (top four panels) onto the first principal component (PC1) (bottom panel) obtained by a seasonally combined EOF analysis of SSTs over the Bering Sea (53°–65°N, 160°E–160°W, shown by boxes in top four panels) The contour interval is 0.1°C, and the absolute values of the regressions larger than 0.5°C are shaded.

total variance. The amplitude is large in summer and small in winter, reflecting the aforementioned pattern of larger interannual variance in summer than in winter (Fig. 2). Also, the correlation coefficients are > 0.7 roughly half of the Bering Sea in summer, but quite small in winter (Fig. 3). The summertime regression pattern is more trapped in the shallow shelf region than the correlations, suggesting that the deep basin and shallow shelf region exhibit qualitatively similar changes with the larger amplitudes in the latter region. Outside the Bering Sea, the SST pattern is a familiar combination of an oval in the central North Pacific and horseshoe along the North American coast with opposite polarities in sign; such SST patterns are observed both on interannual and decadal timescales (e.g., Tanimoto, Iwasaka, Hanawa, & Toba, 1993; Zhang, Wallace & Battisti, 1997; Mantua et al., 1997). The PC1 exhibits a warming trend through the record, with the warmest year in 1997, followed by a sharp cooling until 1999. The warm event in 1997 and associated physical and biological environmental changes attracted considerable attention (e.g. Overland, Bond & Adams, 2001; Stabeno, Bond, Kachel, Salo & Schumacher, 2001; Napp & Hunt, 2001). Similar rapid changes in the PC1 occurred several times in the record. In particular, the cooling in 1946/47 and the warming in 1976/77 are likely to be related to the regime shifts in the 1940s and 1970s (Minobe, 1997; Mantua et al., 1997). After the mid-1970s, the PC1 indicates that the Bering Sea has generally been warm, but prior to the 1970s no clear epoch of the regime lasting 20–30 years is evident. Consequently, decadal variability may have smaller influence in the Bering Sea compared with those over the North Pacific.

The time series of HS in the southern rim of the Bering Sea exhibits similar changes to the SST PC1 after 1970, and the same as true for the deep-basin SLD throughout the available 10-year record (Fig. 4). In particular, all time series captured the warming and sea-level rise from 1995–1997 and subsequent cooling and sea-level fall from 1997–1999. The latter change is likely a part of a pan-Pacific changes described in section 5. The cold anomalies in the early and late 1970s are commonly observed in SST and

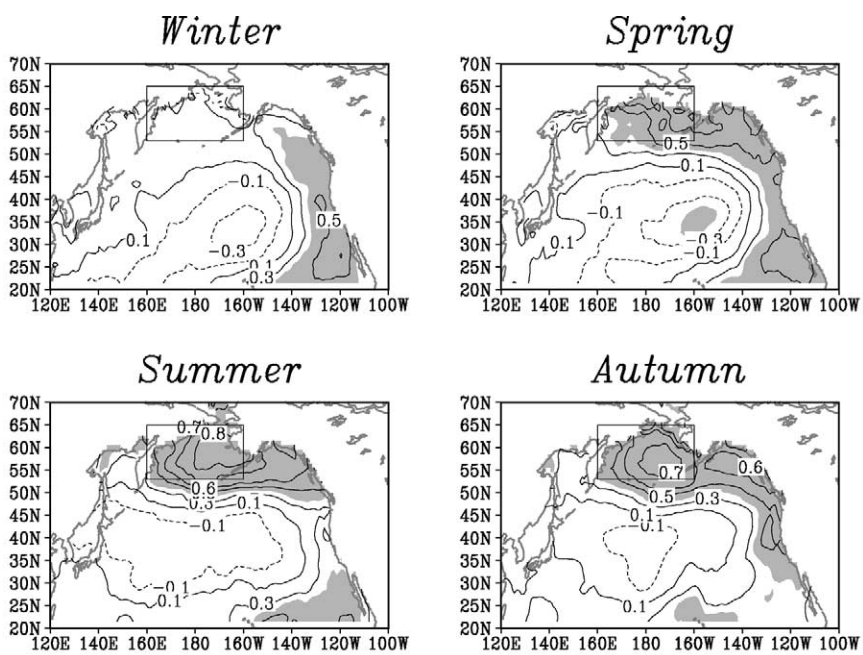

Fig. 3. Same as upper panels of Fig. 2, but for correlation coefficients. Contour intervals are 0.1 (0.2) for the absolute correlations smaller (larger) than 0.5 without zero contour (i.e., ±0.1, 0.3, 0.5, 0.6, 0.7, …), and the absolute values of the correlations larger than 0.4 are shaded.

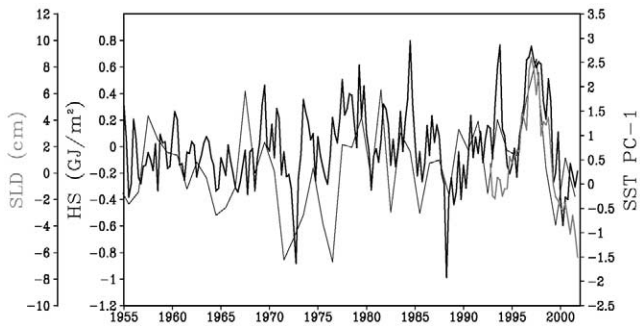

Fig. 4. Seasonally sampled anomalies of HS (thick black line) averaged over the southern rim of the Bering Sea (54°–56°N, 160°E–160°W) and SLD (gray curve) averaged over the deep basin of the Bering Sea (54°–60°N, 160°E–180°) along with the SST PC1 shown in Fig. 2 (thin black line), for the period from 1955–2001. The time series of the SLD averaged over a longitudinal range 160°E–160°W does not changed significantly from the present SLD time series averaged over 160°E–180°, though the quality of the SLD data over the shallow shelf can be questionable as described in section 2.

HS, but relative amplitude of the HS is somewhat smaller. This feature and small amplitudes in the early part of the record in the HS can be an artifact caused by a smaller number of observations, because an optimal interpolation tends to underestimate the amplitudes of anomalies when the numbers of available data are small.

3.2. Sea ice changes

Year-to-year SIC variability in the Bering Sea exhibits strong seasonal dependency, with the strongest variability in spring season followed by winter, consistent with the largest sea-ice extension in spring (Fig. 5). The winter and spring sea-ice variability is generally high over areas where the bathymetry changes from the northeastern shelf to the southwestern deep basin.

Fig. 6 shows correlation coefficients between the SST PC1 and SICs from 1955 to 2001. The correlations are generally negative, and the negative correlations are consistent with a natural relation that warm SSTs are associated with smaller SICs. Consistent with the large amplitudes in the SST EOF-1 shown in Fig. 2, strong correlations are observed in the eastern Bering Sea, with the maximum negative correlation of –0.7 (–0.6) in spring (summer), which explains about half (one third) of the energy of the SIC changes. The region where the absolute correlations are > 0.6 in spring covers the eastern half of the region of large variance shaded in Fig. 5. The sea-ice in the spring season is widely known to be quite important in the intense spring bloom of phytoplankton (e.g. Niebauer, Alexander, & Henrichs, 1990; Niebauer, 1998; Stabeno, Schumacher, Davis & Napp, 1998, 2001).

The time series of SIC in the eastern Bering Sea in the spring season was generally well correlated with the PC1 of the SST from 1955 to 1990 (Fig. 7). However, the warm anomaly in 1997 and cold anomaly in 1999 in the SST were not accompanied by substantial SIC changes, and the large SIC in 1991 occurred independently from the variability of the SST PC1. Thus, the strong relation between the SIC and SST PC1 that was prominent before 1990 is likely to have been be lost during the last decade, and hence the SST and/or SIC might be dominated by mechanisms that were different in the 1990s from those responsible for the changes before 1990. Overland, Bond and Adams (2001) suggested that surface heat flux, especially the summertime short wave radiation, is important for the anomalously warm SSTs in 1997.

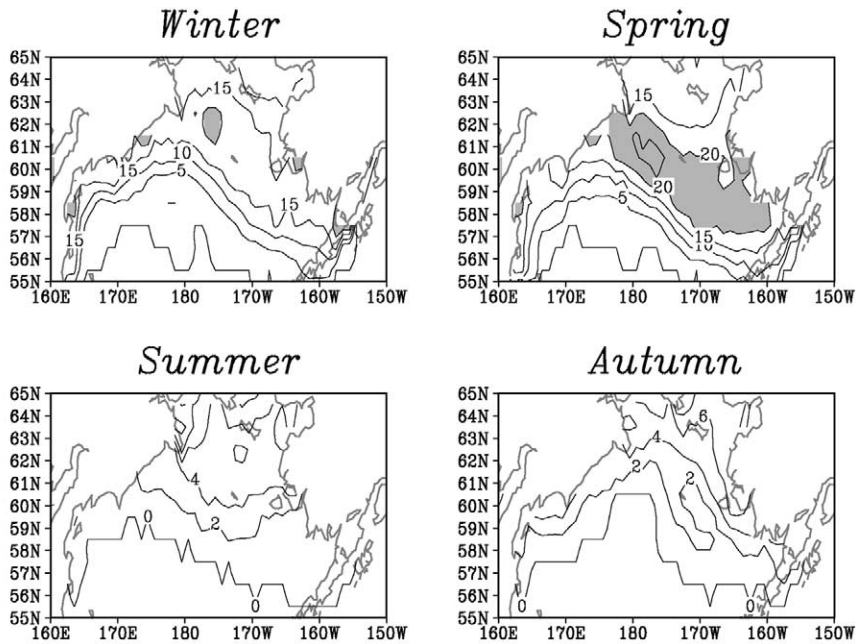

Fig. 5. Standard deviations of SIC anomalies in respective seasons. Contour intervals are 5% in winter and spring seasons, and 2% for summer and autumn seasons. The regions where the standard deviations are larger than 20% are shaded.

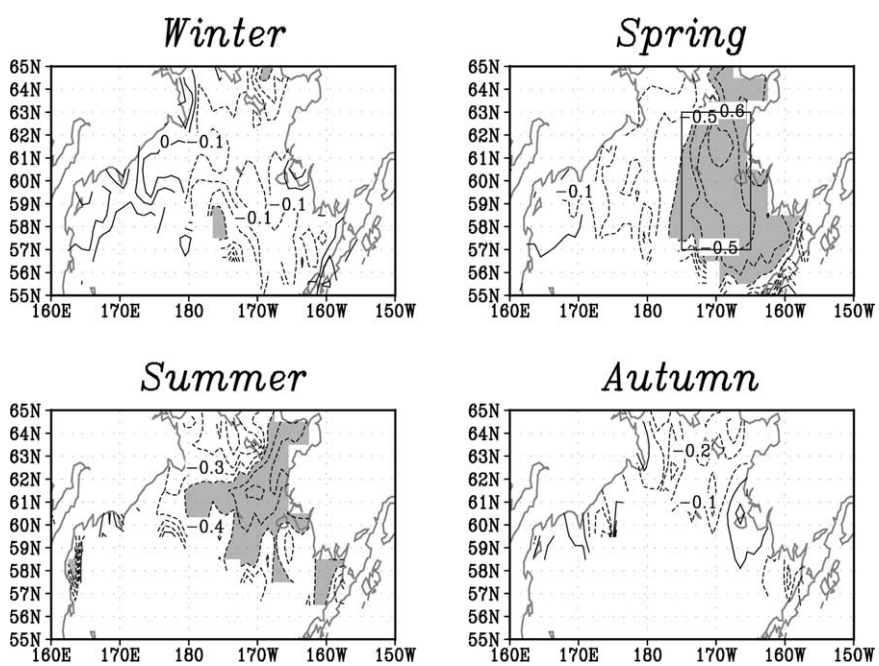

Fig. 6. Correlation coefficients between SICs and the SST PC-1 shown in Fig. 2 for the period from 1955–2001. Contour interval is 0.1, and the absolute values of the correlations larger than 0.4 are shaded. The box in spring panel is the region (175°–165°W, 57°–63°N) where the area-averaged SIC time series shown in Fig. 7 is calculated.

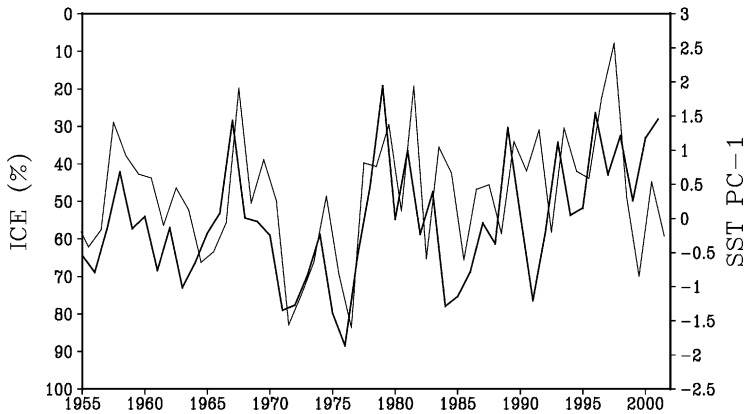

Fig. 7. Area-averaged SIC time series in spring (gray line, left axis with a reversed direction) and the SST PC1 (black line, right axis). The SIC is averaged over the region shown in Fig. 6. The correlation coefficient between two time series is 0.63.

3.3. Atmospheric changes

The changes in the ocean and sea-ice may be caused by atmospheric changes. Hence, we now examine the relationships between the SST PC1 and SLPs. The regression coefficients of the seasonal SLPs onto the SST PC1 exhibit large positive amplitudes over Alaska and negative amplitudes over the northern North Pacific in winter and spring seasons, accompanied by stronger correlations in spring (Fig. 8). This regression pattern suggests that the geostrophic winds, which are qualitatively expressed by SLP gradients, play an important role in SST changes.

As a measure of the southeasterly winds, we calculated the time series of SLP differences between two averaging areas over 60°–70°N, 150°–110°W and over 40°–60°N, 150°E–130°W. The SLP difference agrees qualitatively with the SST PC1 (Fig. 9) and the correlation coefficients between them is as high as 0.60. Therefore, warmer southeasterly anomalous winds are the most likely to play an important role in warmer SSTs in the Bering Sea. The relation between the SST and SLP generally holds throughout the record, and the enhanced and then weakened southeasterly anomalies may have contributed to the warming from 1995–1997 and then the cooling from 1997–1999 in the Bering Sea, although the SLP difference had similar positive anomalies from 1996–1998 without as prominent a peak as was seen in SST PC-1 in year 1997.

The southeasterly winds may also cause smaller SICs. Reynolds, Pease and Overland (1985) reported that sea-ice moves at an angle of 30° to the right of the surface wind direction, suggesting that the southeasterly geostrophic wind can effectively advect sea-ice toward the northwest or the north. The correlation coefficient between the area-averaged SIC shown in Fig. 7 and SLP difference shown in Fig. 9 is 0.50, and explains 25% of the total variance. The present analysis focuses on the seasonal-mean atmospheric condition. This may be related with a shorter events of atmospheric circulations as reported by Overland and Pease (1982), who showed that the maximal sea-ice extent through February to March is closely related with the changes of paths of the cyclones with a high correlation coefficient of 0.71.

4. 1998/99 change over the North Pacific

The Bering Sea cooling and sea-level fall in the late 1990s was accompanied by a series of changes in the physical environment over the North Pacific (Minobe, 2000; Hare & Mantua, 2000; Schwing & Moore,

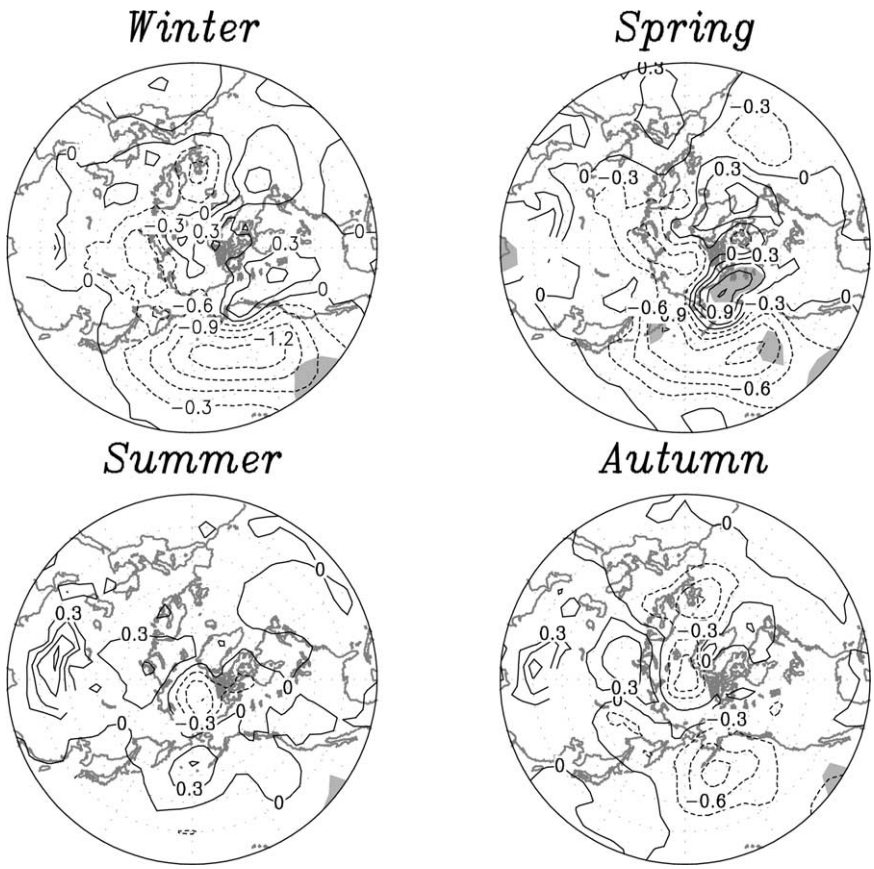

Fig. 8. Regression coefficients of seasonally sampled SLPs onto SST-PC1 shown in Fig. 2 for the period from 1955–2001 in a north polar stereographic map. The contour interval is 0.3 hPa, and the absolute values of the corresponding correlation coefficients larger than 0.4 are shaded. The warmer SSTs are associated with the low SLPs over the northern North Pacific and high SLPs over Alaska in winter and spring seasons, suggesting that the geostrophic wind anomalies, which are proportional to the SLP gradients, play an important role in the SST variability.

2000; Schwing, Murphree, de Witt & Green, 2002). These studies considered the 1998/99 changes in the atmosphere and ocean could be a manifestation of the first major regime shift since the 1970s. Here, we follow the classification for major and minor regime shifts proposed by Minobe (2000), who classified the regime shifts in the 1920s, 1940s and 1970s as major regime shifts, and other changes such as the change in the late 1980s (e.g. Tachibana, Honda, & Takeuchi, 1996; Watanabe & Nitta, 1999; Overland, Adams, & Bond, 1999) as a minor regime shift for the North Pacific sector, based on seasonal persistency and time scales of important oscillations. In view of the possible occurrence of a major regime shift in the 1990s, it is interesting to examine whether or not the changes that occurred in the late 1990s are similar to those of the 1970s. Thus, in this section, we compare the 1998/99 changes over the North Pacific, with those of the 1970s regime shift. Such assessments are useful to understand the differences and similarities between the 1998/99 change and the 1970s climatic regime shift.

Fig. 10 shows the SST and HS difference between 1999–2002 and 1977–1998 as well as the difference between 1977–1998 and 1948–1976 (1965–1976 for HS). The latter being the differences associated with the 1976/77 climatic regime shift. During the 1998/99 change, the mid-latitude central North Pacific exhibited strong warming accompanied by cooling in the eastern and northern North Pacific, both in SST and

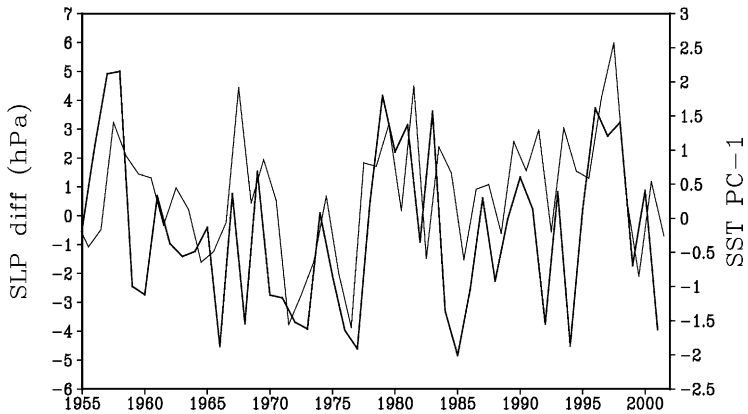

Fig. 9. Time series of an index of southwestern winds expressed by an area-averaged SLP difference (gray line, left axis) given by SLP averaged over 40°–60°N, 150°E–130°W minus SLP over 60°–70°N, 150°–110°W and the SST PC1 (black line, right axis). The correlation coefficient between two time series is 0.60, while the correlation coefficient between the SST PC1 and SLP time series averaged over 60°–70°N, 150°–110W (40°–60°N, 150°E–130°W) is 0.52 (−0.33).

HS. This pattern is similar to the SST and HS changes associated with the 1970s climatic regime shift. However, an interesting difference between the changes of the 1970s and 1990s is that the 1998/99 change involved prominent warming of SSTs in the western North Pacific, whereas the cooling in this region in the 1970s was quite small. The strong warming in the western North Pacific SSTs in the 1990s was common to the 1940s shift (Minobe, 1996). The HS changes in the western North Pacific are observed both in the 1998/99 change and the 1970s regime shift, but HS change in the 1970s was meridionally confined in a narrow region between 35°N and 40°N. The warming in the 1970s is clear in the southeastern Bering Sea, consistent with the high correlation coefficients between the SSTs and PDOI shown in Fig. A-1.

Fig. 11 shows SST and HS time series averaged over three selected regions. Both SST and HS in the central North Pacific and KOE region exhibited dramatic warming in 1998/99 accompanied by rapid cooling in the eastern North Pacific. The cooling is consistent with the earlier reports on coastal SST cooling at Kains Island in British Columbia (McKinnell, Freeland, & Groulx, 1999) and off California (Schwing & Moore, 2000). The cooling and sea-level fall in the Bering Sea (Fig. 4) described above occurred at the same time. Hence all these changes are likely to be features of larger scale oceanic changes over the North Pacific. It is noteworthy that the SST changes in 1998/99 were more rapid than those in the 1970s, both in the KOE and the central North Pacific, and additionally the amplitude of KOE SST was clearly larger in the 1990s than in the 1970s (see Fig. 11).

In the 1970s, cooling in KOE region occurred 4–5 years after the cooling in the central North Pacific, consistent with the previous study by Deser, Alexander and Timlin (1999), who suggested that this lag corresponds to the period over which an oceanic baroclinic Rossby wave propagates from the central North Pacific to KOE region. This phase-lag relation was used for a prediction scheme of the KOE SST (Schneider & Miller, 2001). This relation, however, did not hold for the change in the late 1990s, when the changes occurred almost simultaneously in the KOE and central North Pacific regions, so the prediction scheme would be unsuccessful for this event.

The SLD difference observed by Topex/Poseidon altimetry (Cheney, Miller, Agreen, Doyle & Lillibridge, 1994) between 1999–2001 and 1992–1998 (Fig. 12) exhibited a prominent SLD rise in the central and western Pacific accompanied by SLD fall in the eastern and northern North Pacific, consistent with a series of news releases from the Jet Pollution Laboratory (http://www.jpl.nasa.gov/news/news—index.html, personal communication, Dr. William Patzert). The SLD rise is characterized by strong anomalies at 35°–36°N in a region east of Japan, which is the just north of the mean position of the Kuroshio separation,

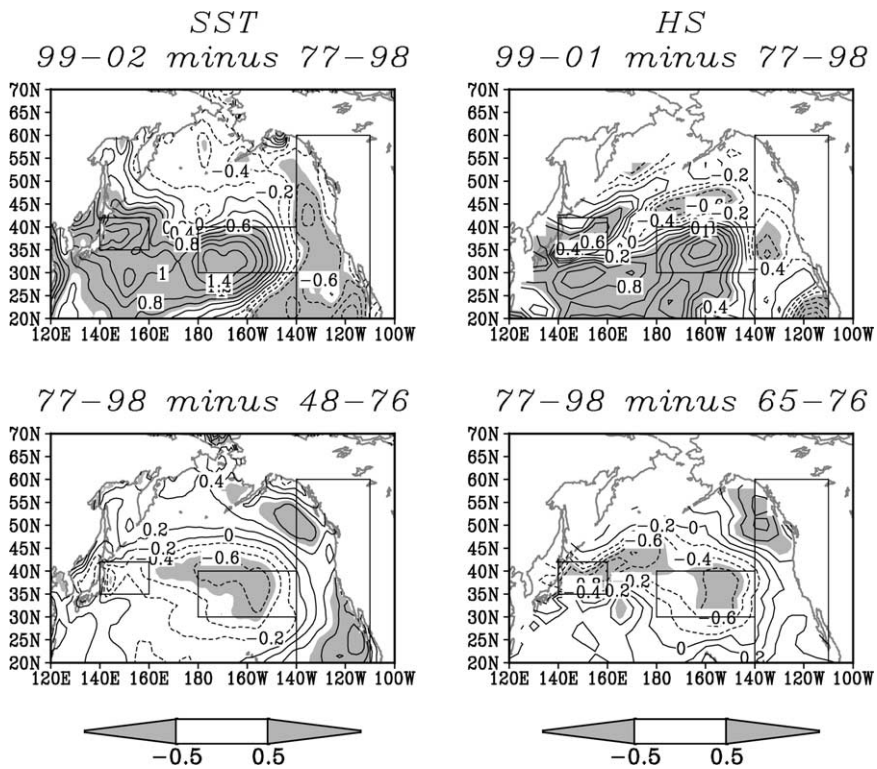

Fig. 10. SST (left panels) and HS (right panels) differences between 1999–2002 (1999–2001 for HS) and 1977–1998 (top panels), and the differences between 1977–1998 and 1948–1976 (1965–1976 for HS) (bottom panels). The reason why the HS used from 1965 is that the unreliable small variability in HS described in section 3.1 (see text). The SST difference between the same periods as the HS (using 1965–1976 instead of 1948–1976) does not significantly change from the present result. The boxes are the regions where area-average time series shown in Fig. 11 are calculated. The regions are the northeastern North Pacific (20°–60°N, 140°–110°W), the central North Pacific (30°–40°N, 180°–140°W), and the Kuroshio and Oyashio Extension (KOE) region (34°–42°N, 140°–160°E).

and a narrow tongue-like structure extending from Japan to the central North Pacific, roughly along the Kuroshio Extension. The tongue-like SLD rise roughly corresponds to the area of HS warming shown in Fig. 10.

From the SLD changes shown in Fig. 12, we can estimate the differences in the surface geostrophic currents between 1999–2001 and 1992–1998 (Fig. 13). The strongest velocity differences are observed just east of Japan, with eastward (westward) anomalies centered around 36°N (34°N), suggesting either the occurrence of warm eddies or a northward migration of the Kuroshio separation. In association with the tongue-like SLD rise, eastward (westward) anomalies are observed from 150°E to 160°W around 33°–35°N (31°–33°N). Including these anomalies, a complex structure with zonal velocity differences of alternating polarities in the meridional direction prevails between 30°N and 45°N. Except for the Kuroshio and Oyashio regions, the largest current anomalies are found as eastward anomalies just to the south of Aleutian Islands, indicating a weakening of the Alaskan Stream. As mentioned above, the Topex/Poseidon SLDs may be problematic at the Aleutian Islands because the tidal modes are unable to represent the energetic tides in the straits. Thus, the postulated weakening of the Alaskan Stream should be checked using other observations such as CTDs or floating buoys. Nevertheless, it is noteworthy that data from a tide gauge at Adak, Alaska (51°52'N, 176°38'W) available from the sea-level data center at University Hawaii exhib-

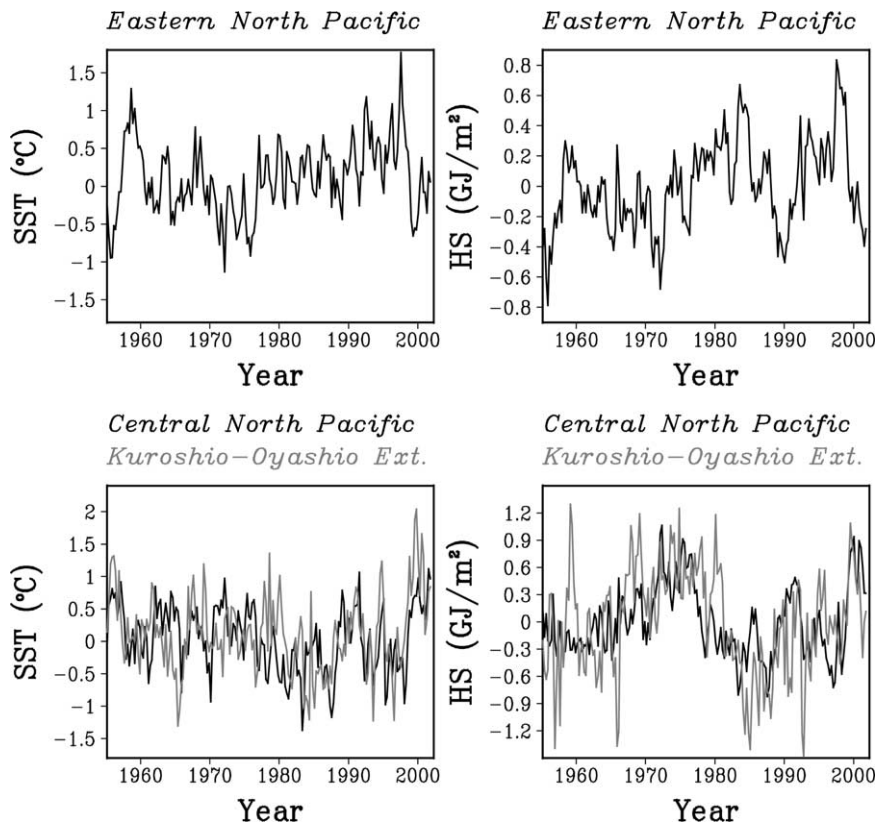

Fig. 11. Seasonal-mean time series of SST (left panels) and HS (right panels) anomalies in the selected region shown in Fig. 10.

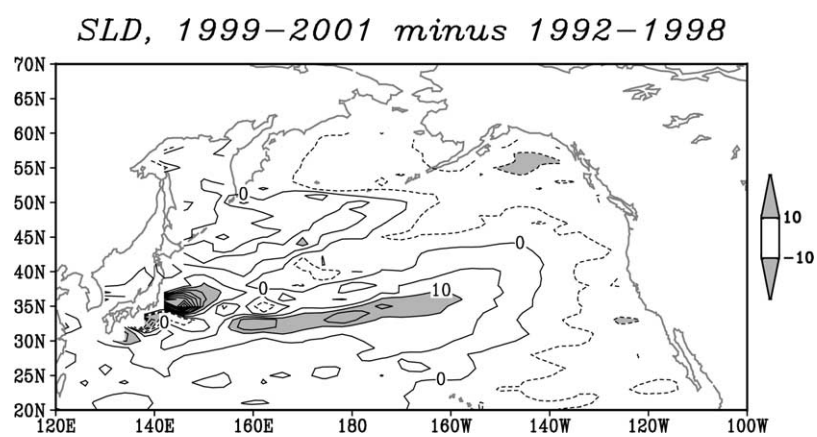

Fig. 12. Differences in SLD between 1999–2001 and 1992–1998. The contour interval is 5 cm, and shades indicate the regions where the SLD difference is larger than 10 cm.

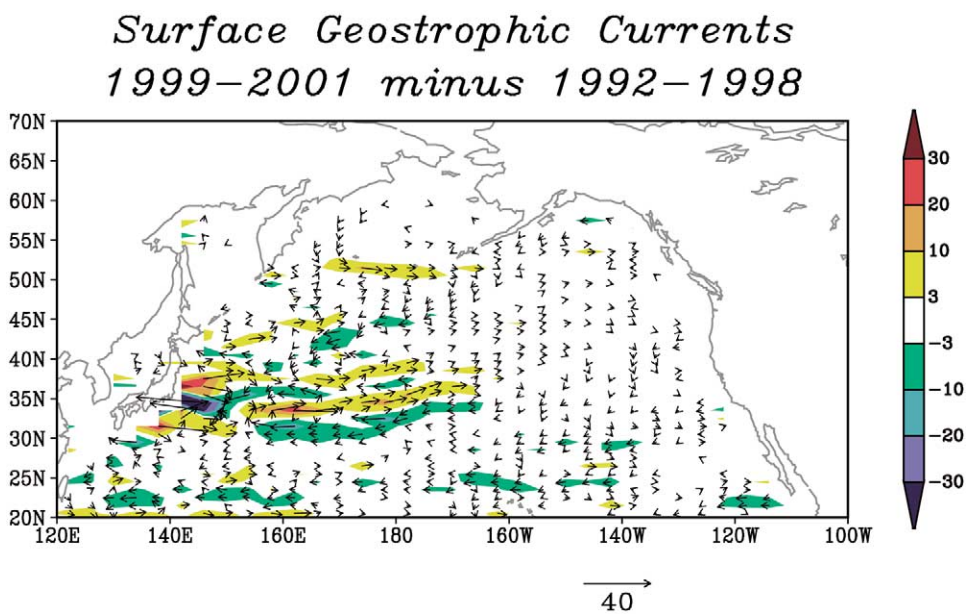

Fig. 13. Surface geostrophic current velocity difference between 1999–2001 and 1992–1998 (arrows), and zonal velocity difference (color). The meridional velocity differences are magnified by two times for an easier visual inspection.

ited similar SLD changes to the Topex/Poseidon SLD throughout the available data period for latter, supporting the SLD decrease at Aleutian Islands in 1998/99.

SLP changes in 1998/99 exhibited a prominent SLP increase centered at 35°N, 155°W (Fig. 14), which is roughly in the same position as the eastern end of the tongue-like SLD rise. It is noteworthy that this SLP center of action is located to the southeast of the SLP difference maximum associated with the 1976/77 climatic regime shift at 50°N, 165°W. The 1998/99 SLP increases in mid-latitudes were accompanied by SLP decreases over Alaska, suggestive of the east Pacific pattern of the atmospheric circulation anomalies aloft.

Anti-cyclonic wind anomalies associated with the positive SLP anomalies cause convergences of Ekman transports, which would further induce the higher SLD with baroclinic structures. The SLD anomalies can propagate westward as a Rossby wave. Thus, the SLD anomalies shown in Fig. 12 were likely to have been caused primarily by surface wind anomalies. However, the simultaneous SLD rise and warming in the SST and HS in the western and central North Pacific cannot be explained by the baroclinic Rossby wave propagation, suggesting that the barotropic response and/or thermohaline forcings played some roles.

5. Summary and discussion

In this paper, the PC1 obtained by the seasonally combined EOF for SSTs over the Bering Sea is used as a representative time series, and its relationships with other parameters including HS, SLD, SIC and SLP have been investigated. Reflecting the largest and smallest interannual variances in SSTs in summer and winter, respectively, the first EOF mode captures the SST variations mainly in summer season. The variation of the PC1 is parallel to the variation of the HS over the southern rim of the Bering Sea after 1970, and also to the variation of the Bering Sea SLD available since 1992. In the 1990s the Bering Sea

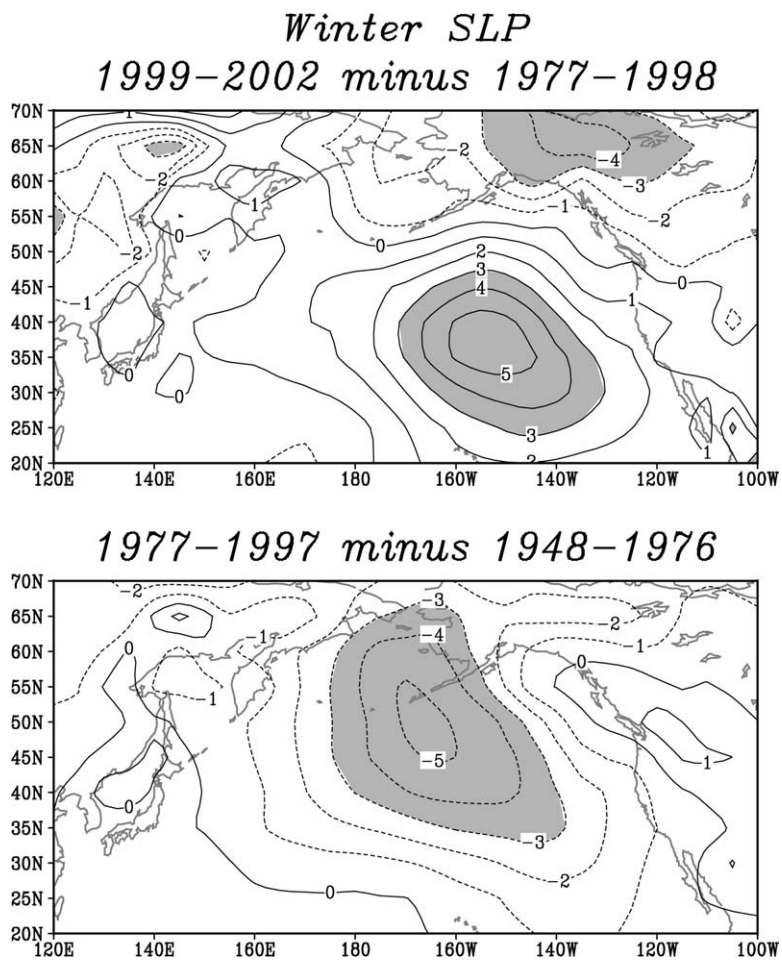

Fig. 14. Wintertime SLP differences between 1999–2002 and 1977–1998 (top panel) and differences between 1977–1998 and 1967–1976 (bottom panel). Contour interval is 1 hPa, and shades indicate the regions where the SLP differences are larger than 3 hPa.

experienced energetic changes; water temperatures warmed from 1995–1997 accompanied by a sea-level rise, followed by cooling and sea-level fall from 1997–1999.

High correlations between the SICs in the eastern Bering Sea and SST PC1 were found in spring. The time series comparison showed that a good relation between them existed only prior to 1990. The relation between the SST PC1 and atmospheric circulation represented by SLPs was also most prominent in spring season. The spring geostrophic wind anomalies in northwest-southeast direction are likely to influence the SST PC1, which has the largest contribution in summer, and also SICs in spring, via advections of air or water or ice. It should be interesting in future to examine using numerical models, the possibility that the springtime SIC anomalies' function as a memory, influencing the summertime SST anomalies. Stabeno, Bond, Kachel, Salo and Schumacher (2001) also noted the possibility that the sea-ice may transmit information of wintertime atmospheric forcings to summertime SSTs.

The southwesterly wind anomalies are likely to have played an important role in the warming from 1995–1997 and cooling from 1997–1999 in the Bering Sea. However, how the HS and SLD responded to these wind anomalies or other forcings is unknown, and the mechanism leading to the whole sequence of the Bering Sea changes needs be clarified in future studies.

The 1998/99 change was not unique to the Bering Sea, since SSTs and HSs simultaneously and abruptly increased throughout the central North Pacific and KOE regions accompanied by cooling in the eastern North Pacific. These changes may be related to the possibility that a major regime shift occurred in 1998/1999, which, if it subsequently proves to have been the case, will have been the first major regime shift after the 1970s regime shift, as discussed by Minobe (2000); Hare and Mantua (2000); Schwing and Moore (2000) and Schwing, Murphree, de Witt, & Green (2002).

For the 1998/99 change, Topex/Poseidon altimetry has provided useful information for monitoring the variability in the Bering Sea and the North Pacific. The SLD change is characterized by an SLD rise in the regions of around the Kuroshio separation and Kuroshio extension with a tongue-like structure and by SLD fall in the Bering Sea and the eastern North Pacific, consistent with the HS difference. The associated surface velocity differences exhibit a complex structure, including the eastward (westward) anomalies around 35°–36°N (34°–35°N) just east of Japan and along the northern (southern) flanks of the tongue-like SLD rise and weakening anomalies of the Alaskan Stream.

The ongoing atmospheric and oceanic anomalies starting from the late 1990s have had substantial impacts on a number of physical parameters. Some of those changes have been shown in this paper, and others have been described in Minobe (2000); Hare and Mantua (2000) and Schwing and Moore (2000). A critical question is, of course, whether or not the 1998/99 change signals a regime shift; a question that the author believes that, presently, we do not understand the nature and mechanism of the regime shifts deeply enough to answer. We have neither the ability to *forecast*, nor confidently *nowcast*, and even *hindcast*, a regime shift within four years of its occurrence. However, it is interesting to discuss further how we can interpret the affect of the 1998/99 change in the near future based on today's knowledge. There are three possible hypotheses for the explanation of the nature of the 1998/99 change:

1. the main body of the 1998/1999 change was the result of interannual variability
2. the 1998/1999 change was associated with the decadal-interdecadal variability, but dib not result from a major regime shift, which involves a 20–30 year lasting regime, or
3. the 1998/1999 change was indeed a major regime shift.

To distinguish hypothesis (i) from the others, we will need to wait for another a few years of data accumulation. Given the fact that one of the major timescales of the influence of the ENSO on mid-latitudes is 5–6 years (e.g., Zhang, Sheng, & Shabbar, 1998), by the year 2003/04 we will have accumulated sufficient data to allow us to determine whether the 1998/1999 change was associated with the interannual variability or not. However, distinguishing between the hypotheses (ii) and (iii) is a more difficult problem, for which it is necessary to understand the mechanism of the regime shifts, and to be able to identify the fingerprints of a regime shift that are essential for the mechanism. Although a number of papers have proposed a mechanism for decadal–interdecadal oscillations on timescales of 10–30 years over the North Pacific as summarized in Miller and Schneider (2000); Minobe (2000), and Mantua and Hare (2002), still there is no accepted hypothesis to explain regimes lasting 20–30 years for the Pacific climate. The theoretical and numerical studies for the multidecadal timescales of the Pacific climate changes are, therefore, quite important, and this importance is enhanced by the possibility that there was a major regime shift in 1998/99.

Acknowledgements

I thank U. Batt, A. Miller, N. Mantua, and F. B. Schwing for preprints, and N. Mantua for Pacific Decadal Oscillation Index, D. Thompson for Arctic Oscillation Index, P. D. Jones for Southern Oscillation Index. Constructive comments from anonymous reviewers have been helpful in improving this paper. Some

figures have been produced with the GrADS package developed by B. Doty. This study is supported by grants from the Japanese Ministry of Education, Culture and Science.

Appendix A

For convenience of the readers who are interested in relationships between the large scale climate indices and Bering Sea SST or SICs, here simultaneous correlation maps are plotted with respect to Pacific Decadal Oscillation Index (PDOI), North Pacific Index (NPI), Arctic Oscillation Index (AOI), and Southern Oscillation Index (SOI) in each of four seasons using the data from 1955 to 2001 for SSTs in Fig. A-1 and for SICs in Fig. A-2, respectively.

The PDOI is the leading PC of monthly SST anomalies in the North Pacific Ocean, poleward of 20°N (Zhang, Wallace & Battisti, 1997; Mantua, Hare, Zhang, Wallace & Francis, 1997). The monthly mean

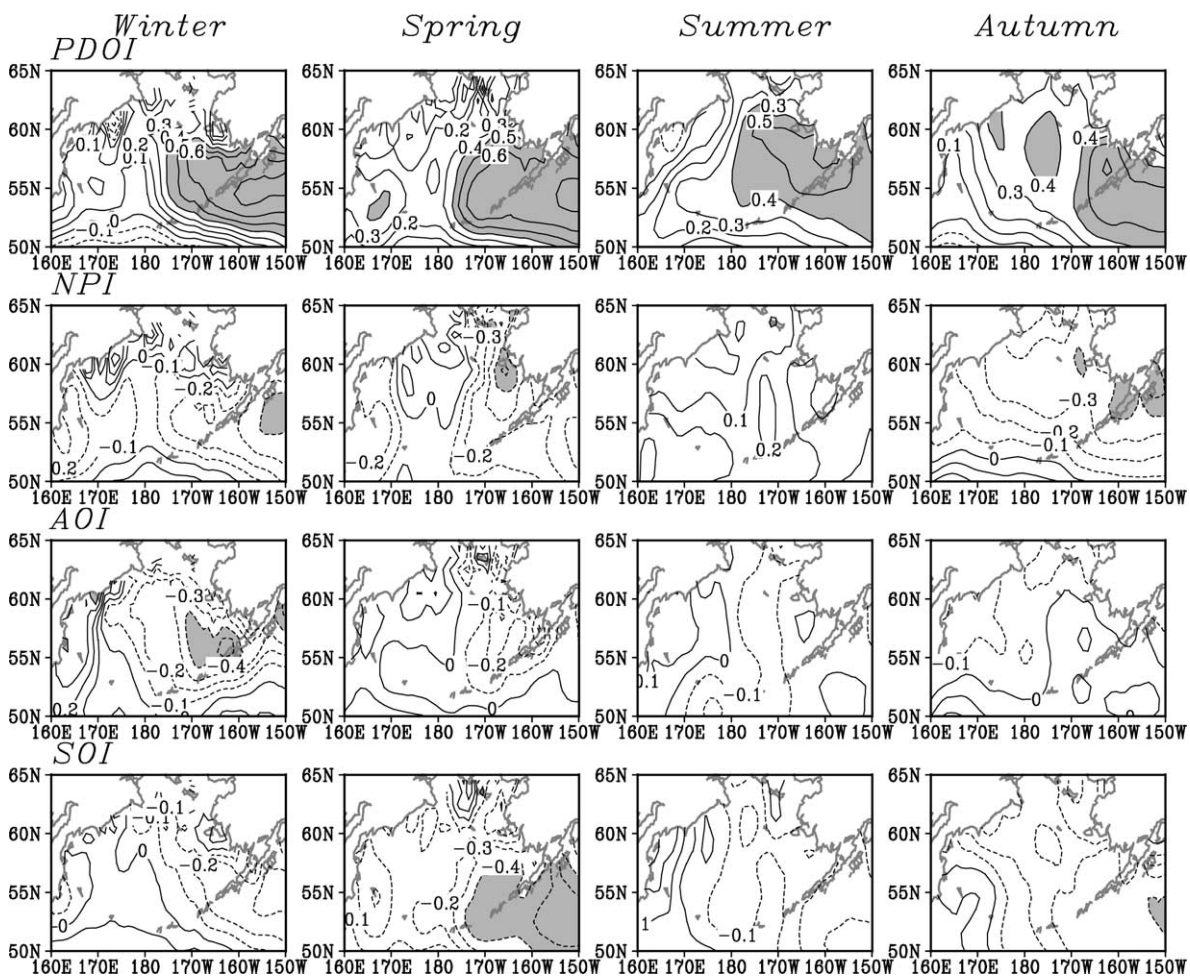

Fig. A-1 Simultaneous correlation coefficients of SSTs with respect to the Pacific Decadal Oscillation Index (PDOI), North Pacific Index (NPI), Arctic Oscillation Index (AOI), and Southern Oscillation Index (SOI) in each season. A column corresponds to a season, and a row corresponds to a climate index. Contour interval is 0.1, and the absolute values of the correlations larger than 0.4 are shaded.

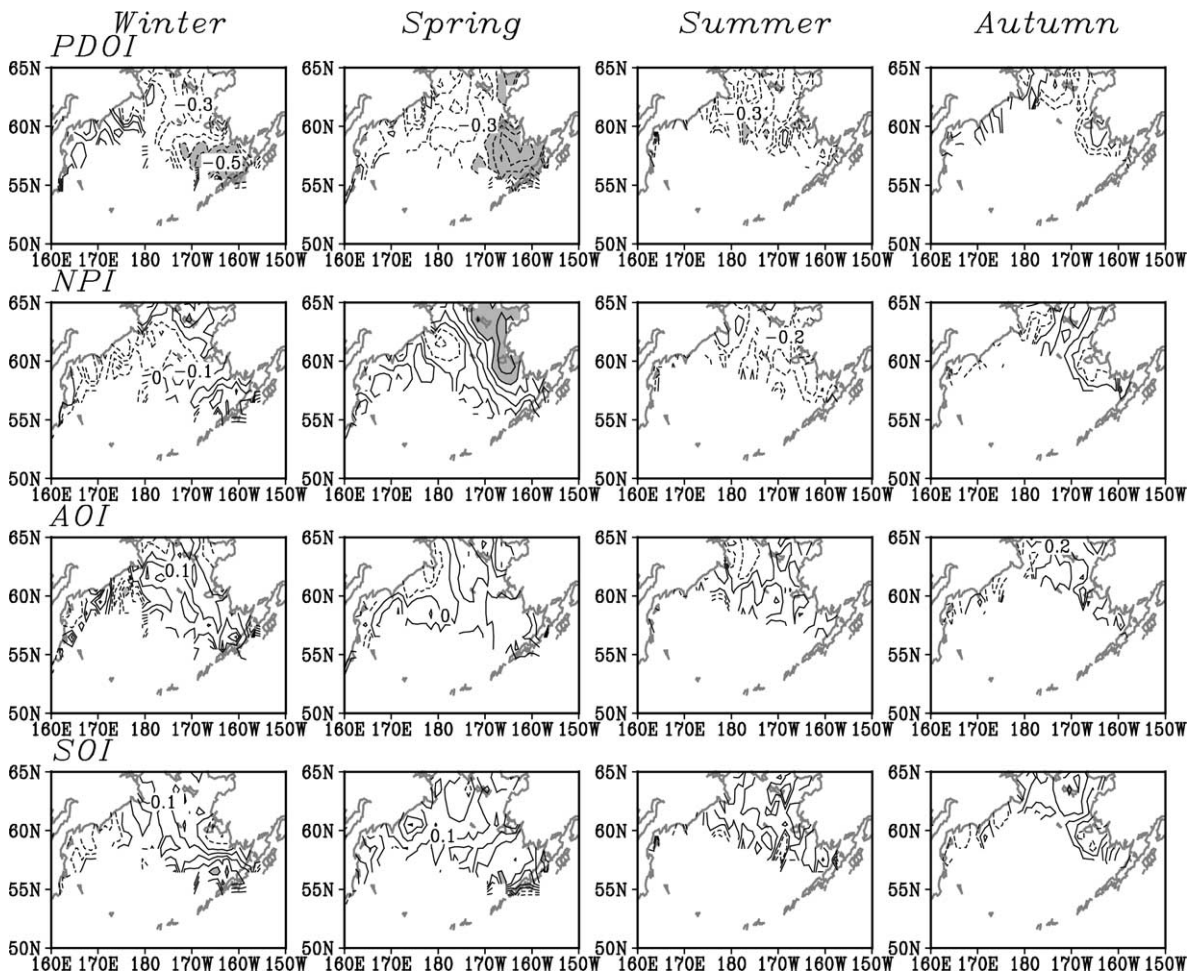

Fig. A-2 Same as Fig. A1, but for SICs.

global average SST anomalies are removed to separate this pattern of variability from any *global warming* signal that may be present in the data.

The other three indices are based on SLPs. The NPI is defined by Trenberth and Hurrel (1994) as an area-weighted SLP average over 30°–65°N, 160°E–140°W. The NPI is highly correlated with the leading PC of the 500 hPa geopotential height with the associated EOF of a PNA pattern (Trenberth and Hurrel, 1994), and correlated with the leading PC of the winter SLP anomalies in the North Pacific (Minobe & Mantua 1999) The Arctic Oscillation (AO) was proposed by Thompson & Wallace (1998), and the Arctic Oscillation index is the leading EOF mode of monthly SLPs north of 20°N, calculated based on the NCAR SLP before 1958 and NCEP/NCAR reanalysis (Kalnay et al., 1996) after that. The SOI is defined as the sea-level pressure at Tahiti minus that at Darwin, and has been provided by P.D. Jones.

The correlations between the SSTs and PDOI are distinctively higher than those for other climate indices. However, this should not be too emphasized, because the PDOI is calculated using the SSTs over the North Pacific including the Bering Sea, but other indices are calculated from the SLPs. It should be noted that even those high correlations with the PDOI cover only a fraction of the Bering Sea, with maximal correlations of 0.6, indicating that this relationship only explains about one third of the variance in part

of the Bering Sea. The resultant area-averaged explained variance of the Bering Sea SST due to the PDOI is in a range between 11% in autumn and 20% in spring.

References

Cheney, R., Miller, L., Agreen, R., Doyle, N., & Lillibridge, J. (1994). TOPEX/POSEIDON: The 2-cm solution. *Journal of Geophysical Research, 99*, 24.

Deser, C., Alexander, M. A., & Timlin, M. S. (1999). Evidence for a wind-driven intensification of the Kuroshio Current extension from the 1970s to 1980s. *Journal of Climate, 12*, 1697–1706.

Eanes, R., & Bettadpur, S. (1996). The CSR3.0 global ocean tide model: Diurnal and semi-diurnal ocean tides from TOPEX/POSEIDON altimetry, CSR-TM-96-05, University of Texas, Center for Space Research, Austin, TX.

Hare, S. R., & Mantua, N. J. (2000). Empirical evidence for North Pacific regime shifts in 1977 and 1989. *Progress in Oceanography, 47*, 103–146.

Kalnay, E., Kanamitsu, M., Kistler, R., Collins, W., Deaven, D., Gandin, L., Iredell, M., Saha, S., White, G., Woollen, J., Zhu, Y., Leetmaa, A., Reynolds, B., Chelliah, M., Ebisuzaki, W., Higgins, W., Janowiak, J., Mo, K. C., Ropelewski, C., Wang, J., Jenne, R., & Joseph, D. (1996). The NCEP/NCAR 40-year reanalysis project. *Bulletin of American Meteorological Society, 77*, 437–472.

Mantua, N. J., Hare, S. R., Zhang, Y., Wallace, J. M., & Francis, R. C. (1997). A Pacific interdecadal climate oscillation with impacts on salmon production. *Bulletin of American Meteorological Society, 76*, 1069–1079.

Mantua, N. J., & Hare, S. R. (2002). The Pacific Decadal Oscillation. *Journal of Oceanography, 58*, 35–44.

Miller, A. J., & Schneider, N. (2000). Interdecadal climate regime dynamics in the North Pacific Ocean: Theories, observations and ecosystem impacts. *Progress in Oceanography, 47*, 355–379.

Minobe, S. (1996). Interdecadal temperature variation of deep water in the Japan Sea (East Sea). In *Proceedings of the Fourth CREAMS workshop, Vladivostok, Russia* (pp. 81–88).

Minobe, S. (1997). A 50–70 year climatic oscillation over the North Pacific and North America. *Geophysical Research Letters, 24*, 683–686.

Minobe, S., & Mantua, N. (1999). Interdecadal modulation of interannual atmospheric and oceanic variability over the North Pacific. *Progress in Oceanography, 43*, 163–192.

Minobe, S. (2000). Spatio-temporal structure of the pentadecadal variability over the North Pacific. *Progress in Oceanography, 47*, 99–102.

Napp, J. M., & Hunt, G. L. (2001). Anomalous conditions in the southeastern Bering Sea,7: linkages among climate, weather, ocean, and biology. *Fisheries Oceanography, 10*, 61–68.

Niebauer, H. J. (1988). Effects of El Niño-Southern Oscillation and North Pacific weather patterns on interannual variability in the subarctic Bering Sea. *Journal of Geophysical Research, 93*, 5051–5068.

Niebauer, H. J. (1998). Variability in Bering Sea ice cover as affected by a regime shift in the North Pacific in the period 1947–96. *Journal of Geophysical Research, 103*, 27.

Niebauer, H. J., Alexander, V., & Henrichs, S. (1990). Physical and biological interaction in the spring bloom at the Bering Sea marginal ice edge zone. *Journal of Geophysical Research, 95*, 22.

Overland, J. E., & Pease, C. E. (1982). Cyclone climatology of the Bering Sea and its relation to sea ice extent. *Monthly Weather Review, 110*, 5–13.

Overland, J. E., Adams, J. M., & Bond, M. A. (1999). Decadal variability of the Aleutian low and its relation to high-latitude circulation. *Journal of Climate, 12*, 1542–1548.

Overland, J. E., Bond, N. A., & Adams, J. M. (2001). North Pacific atmospheric and SST anomalies in 1997: Links to ENSO? *Fisheries Oceanography, 10*, 69–80.

Parker, D. E., & Jackson, M. (1995). Marine surface temperature: Observed variations and data requirements. *Climatic Change, 31*, 559–600.

Rayner, N. A., Horton, E. B., Parker, D. E., Folland, C. K., & Hackett, R. B., (1996). Version 2.2 of the global sea ice and sea surface temperature data set, 1903-1994. CRTN44, Available from Hadley Center, Meteorological Office, Bracknell, UK.

Reynolds, M., Pease, C. H., & Overland, J. E. (1985). Ice drift and regional meteorology in the southern Bering Sea: Results from MIZEX west. *Journal of Geophysical Research, 90*, 11967–11981.

Schneider, N., & Miller, A. J. (2001). Predicting western North Pacific ocean climate. *Journal of Climate, 14*, 3997–4002.

Schwing, F. B., & Moore, C. S. (2000). A year without summer for California, or a harbinger of a climate shift? *EOS, Transaction, American Geophysical Union, 81*, 301–305.

Schwing, F. B., Murphree, T., de Witt, L., & Green, P. (2002). The evolution of oceanic and atmospheric anomalies in the Northeast Pacific during the El Niño and La Niña events of 1995–2001. *Progress in Oceanography, 54*, 459–491.

Shum, C. K., Woodworth, P. L., Andersen, O. B., Egbert, G. D., Francis, O., King, C., Klosko, S. M., Provost, C. Le, Li, X., Molines,

J. -M., Parke, M. E., Ray, R. D., Schlax, M. G., Stammer, D., Tierney, C. C., Vincent, P., & Wunsch, C. I. (1997). Accuracy assessment of recent ocean tide models. *Journal of Geophysical Research*, *102*, 25173–25194.

McKinnell, S., Freeland, H. J., & Groulx, S. D. (1999). Assessing the northern diversion of sockeye salmon return to the Fraser River, BC. *Fisheries Oceanography*, *8*, 104–114.

Stabeno, P. J., Schumacher, J. D., Davis, R. F., & Napp, J. M. (1998). Under-ice observations of water column temperature, salinity and spring phytoplankton dynamics: Eastern Bering Sea shelf. *Journal of Marine Research*, *56*, 239–255.

Stabeno, P. J., Bond, N. A., Kachel, N. B., Salo, S. A., & Schumacher, J. D. (2001). On the temporal variability of the physical environment over the south-eastern Bering Sea. *Fisheries Oceanography*, *10*, 81–98.

Tachibana, Y., Honda, M., & Takeuchi, K. (1996). The abrupt decrease of the sea ice over the southern part of the Sea of Okhotsk in 1989 and its relation to the recent weakening of the Aleutian low. *Journal of Meteorological Society Japan*, *74*, 579–584.

Tanimoto, Y., Iwasaka, N., Hanawa, K., & Toba, Y. (1993). Characteristic variation of sea surface temperature with multiple time scale in the North Pacific. *Journal of Climate*, *6*, 1153–1160.

Trenberth, K. E., & Paolino, D. A. (1980). The Northern Hemisphere sea-level pressure data set: Trends, errors, and discontinuities. *Monthly Weather Review*, *108*, 855–872.

Trenberth, K. E., & Hurrell, J. W. (1994). Decadal atmosphere-ocean variations in the Pacific. *Climate Dynamics*, *9*, 303–319.

Trenberth, K. E., & Caron, J. M. (2000). The Southern Oscillation revisited: Sea level pressures, surface temperatures, and precipitation. *Journal of Climate*, *13*, 4358–4365.

Walsh, J. E., & Johnson, C. M. (1979). An analysis of Arctic sea ice fluctuations, 1953–77. *Journal of Physical Oceanography*, *9*, 580–591.

Walsh, J. E., (1995). A sea ice database. In Folland, C. K. and D. P. Rowell, (Eds), *Workshop on simulations of the climate of the twentieth century using GISST*, 28-30 November 1994, Hadley Centre, Bracknell, UK, 54-55, Meteorological Office, London Road, Bracknell, Berkshire, RG12 2SY. Hadley Centre for Climate Prediction and Research. CRTN 56.

Watanabe, M., & Nitta, T. (1999). Decadal changes in the atmospheric circulation and associated surface climate variations in the northern hemisphere winter. *Journal of Climate*, *12*, 494–510.

White, W. B. (1995). Design of a global observing system for gyre-scale upper ocean temperature variability. *Progress in Oceanography*, *36*, 169–217.

Zhang, Y., Wallace, J. M., & Battisti, D. S. (1997). ENSO-like interdecadal variability: 1900–1993. *Journal of Climate*, *10*, 1004–1020.

Zhang, X., Sheng, J., & Shabbar, A. (1998). Modes of interannual and interdecadal variability of Pacific SST. *Journal of Climate*, *11*, 2556–2569.